J|A|C|S ARTICLES

Published on Web 09/24/2010

Understanding the Structure and Formation of Uranyl Peroxide Nanoclusters by Quantum Chemical Calculations

Bess Vlaisavljevich,[†] Laura Gagliardi,*[,†] and Peter C. Burns*[,‡]

Department of Chemistry, University of Minnesota, and Supercomputing Institute, 207 Pleasant St. SE, Minneapolis, Minnesota 55455, and Department of Civil Engineering and Geological Sciences and Department of Chemistry and Biochemistry, University of Notre Dame, Notre Dame, Indiana 46556

Received June 17, 2010; E-mail: gagliard@umn.edu; pburns@nd.edu

Abstract: Quantum chemical calculations were performed to understand the formation of nanoscale cage clusters based on uranyl ions. We investigated the uranyl−peroxide−uranyl interaction and compared the geometries of clusters with and without such interactions. We show that a covalent interaction along the $U-O_{peroxo}$ bonds causes the $U-O_2-U$ dihedral angle to be bent, and it is this inherent bending of the configuration that encourages curvature and cage cluster formation. The $U-O_2-U$ dihedral angle of the peroxo bridge is tuned by the size or electronegativity of the counterion present.

Introduction

Hexavalent uranium, as the linear $(UO_2)^{2+}$ uranyl ion,[1] is central to the chemistry of this element. We previously reported 13 nanoscale cage clusters that are based on uranyl ions.[2−7] This class of polyoxometalates self-assembles in aqueous solutions under ambient conditions. The uranyl ions are in hexagonal bipyramidal polyhedra with O atoms of the uranyl ions at their apexes. Each bipyramid shares three equatorial edges with other bipyramids, with two or three of these shaded edges corresponding to peroxide groups. These cage clusters are a major departure from the extended sheets that normally result from linkage of uranyl bipyramids.[8,9] Their creation requires circumventing the sheet-forming tendencies of the polyhedra to cause curvature. We argued such curvature arises because the uranyl−peroxide−uranyl interaction is inherently bent.[4] Here we examine the quantum chemical details of this interaction.

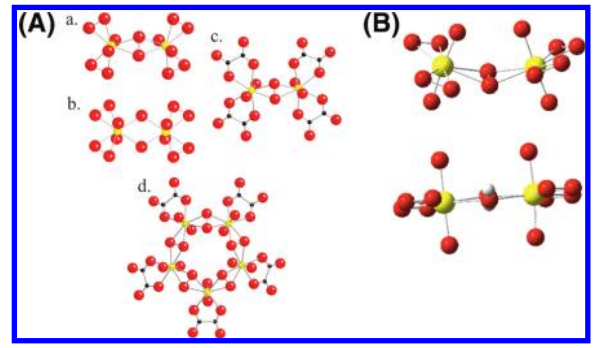

Figure 1. (A) Model clusters derived from experimentally determined crystal structures. (a) $[(UO_2)_2(O_2)_5]^{6-}$, designated 2U−P as shown and 2U−P−A with counterions A added. (b) $[(UO_2)(O_2)_2(OH)]_2^{6-}$, designated 2U−OH−A with counterions added. (c) $[(UO_2)_2(O_2)(C_2O_4)_4]^{6-}$, designated 2U−P−Ox−A with counterions added. (d) $[(UO_2)(O_2)(C_2O_4)]_5^{10-}$, designated 5U−P−Ox−A with counterions added. Calculations were also done for a hypothetical cluster with composition $[(UO_2)_2(OH)_2(C_2O_4)_4]^{6-}$ derived from structure c by replacing the peroxo by two hydroxo ions. This is designated 2U−OH−Ox−A with counterions added and 2U−OH−A−H_2O with two H_2O groups added. U, yellow; O, red; C, black. (B) Enlarged picture of the peroxo structure (structure a in panel A) versus hydroxo structure (structure b in panel A), where the bending of the peroxo is emphasized.

We have conducted computational studies of the uranyl−peroxide−uranyl interaction and compared the geometries of clusters with and without such interactions. Several clusters isolated in crystal structures provide the starting points for our work (Figure 1). The cluster $[(UO_2)_2(O_2)_5]^{6-}$ is from $Na_2Rb_4(UO_2)_2(O_2)_5(H_2O)_{14}$[10] and contains two uranyl hexagonal bipyramids that share a peroxide edge. Each bipyramid has two additional peroxide edges. The $U-O_2-U$ dihedral angle is 153.1°. For comparison, the cluster $[(UO_2)(O_2)_2(OH)]_2^{6-}$, from $K_6[(UO_2)(O_2)_2(OH)]_2(H_2O)_7$,[10] contains two hexagonal bipyramids with a shared edge that is two hydroxyl groups. The

[†] Department of Chemistry, University of Minnesota, and Supercomputing Institute.

[‡] University of Notre Dame.

(1) Morss, L. R.; Edelstein, N. M.; Fuger, J.; Katz, J. J. *The Chemistry of the Actinide and Transactinide Elements*; Springer: Dordrecht, The Netherlands, 2006.
(2) Burns, P. C.; Kubatko, K. A.; Sigmon, G.; Fryer, B. J.; Gagnon, J. E.; Antonio, M. R.; Soderholm, L. *Angew. Chem., Int. Ed.* **2005**, *44*, 2135–2139.
(3) Forbes, T. Z.; McAlpin, J. G.; Murphy, R.; Burns, P. C. *Angew. Chem., Int. Ed.* **2008**, *47*, 2824–2827.
(4) Sigmon, G.; Ling, J.; Unruh, D. K.; Moore-Shay, L.; Ward, M.; Weaver, B.; Burns, P. C. *J. Am. Chem. Soc.* **2009**, *131*, 16648–16649.
(5) Sigmon, G. E.; Unruh, D. K.; Ling, J.; Weaver, B.; Ward, M.; Pressprich, L.; Simonetti, L.; Burns, P. C. *Angew. Chem., Int. Ed.* **2009**, *48*, 2737–2740.
(6) Sigmon, G. E.; Weaver, B.; Kubatko, K. A.; Burns, P. C. *Inorg. Chem.* **2009**, *48*, 10907–10909.
(7) Unruh, D. K.; Burtner, A.; Pressprich, L.; Sigmon, G.; Burns, P. C. *Dalton Trans.* **2010**, *39*, 5807–5813.
(8) Burns, P. C. *Can. Mineral.* **2005**, *43*, 1839–1894.
(9) Burns, P. C.; Ewing, P. C.; Hawthorne, F. C. *Can. Mineral.* **1997**, *35*, 1551–1570.
(10) Kubatko, K. A.; Forbes, T. Z.; Klingensmith, A. L.; Burns, P. C. *Inorg. Chem.* **2007**, *46*, 3657–3662.

U−$(OH)_2$−U dihedral angle is 180°. The cluster $[(UO_2)_2(O_2)(C_2O_4)_4]^{6-}$, from $K_6[(UO_2)_2(O_2)(C_2O_4)_4]$,[4] contains two uranyl hexagonal bipyramids with a shared peroxide equatorial edge. The remaining two equatorial edges of each bipyramid are defined by bidentate oxalate groups. The U−O_2−U dihedral angle is 152.9°. A larger cluster with composition $[(UO_2)(O_2)(C_2O_4)]_5^{10-}$ is from $K_{10}[(UO_2)(O_2)(C_2O_4)]_5(H_2O)_{13}$.[4] It consists of a five-membered ring of bipyramids, and the shared edges are peroxide groups. Again, each bipyramid contains one bidentate oxalate group. The dihedral angles of the U−O_2−U bridges range from 137.5° to 144.5°.

Theoretical Calculations

Calculations were performed by density functional theory (DFT) and multiconfigurational methods (CASSCF/CASPT2) for the experimentally observed clusters as well as for a hypothetical cluster derived from $[(UO_2)_2(O_2)(C_2O_4)_4]^{6-}$ by replacing the peroxide group shared between the uranyl ions with two hydroxyl groups. Full geometry optimizations were performed without imposing any symmetry constraint. The starting structures were were taken from experiment, when available. Counterions were evently distributed around these starting structures for each cluster. All systems under consideration have a singlet spin state as the ground state.

Density functional theory (DFT) geometry optimizations of the experimentally synthesized clusters were performed with the Perdew−Burke−Ernzerhof (PBE) exchange−correlation functional[11] and triple-ζ valence plus polarization (def-TZVP)[12] basis sets on all atoms. Quasirelativistic pseudopotentials were used for U atoms, with 60 core electrons.[13,14] The TURBOMOLE 5.10 program package was employed.[15,16]

Multiconfigurational complete active space (CASSCF)[17] calculations followed by second-order perturbation theory (CASPT2)[18] were performed at the DFT optimized geometries of 2U−P−Na and 2U−P−Ox−Na. Both systems are essentially single-configurational. However, in the peroxo cases, the molecular orbitals are more delocalized than in the hydroxo cases. Scalar relativistic effects were included by use of the Douglas−Kroll−Hess[19] Hamiltonian and the relativistic all-electron ANO-RCC basis sets with double-ζ quality (ANO-RCC-VDZP)[20] with the following contractions: [8s 7p 5d 3f 1g] for U and [3s 2p 1d] for O and C. The ANO-RCC-MB basis set was employed for H with a contraction of [1s]. Several active spaces were tested. An ideal active space for a single uranyl ion would include 12 electrons in 12 orbitals (see for example ref 21). In the diuranyl compound, one should have 24 electrons in 24 orbitals in the active space, and this would still not describe the interaction with the two uranyls and the peroxo unit. We have thus decided to include only the highest occupied−lowest unoccupied molecular orbital (HOMO−LUMO) uranyl-based orbitals, namely, the bonding and antibonding σ_u orbitals and the orbitals describing the interaction between U and the bridging peroxo. In total, the active space contains eight electrons in eight orbitals. Four of them are the uranyl bonding and antibonding orbitals and four of them are the U−O(peroxo) bonding orbitals, which are linear combinations of the 7s, 6d, and 5f orbitals of U and 2p of O. Including the nonbonding U 5f-based orbitals in the active space does not have an effect. It is sufficient to correlate them in the subsequent CASPT2 treatment. For the pentauranyl complex we have not performed CASSCF/CASPT2 calculations because a system with five U atoms is prohibitively large to be treated with this method.

Explicit water molecules and a reaction field Hamiltonian were included in some of the calculations in order to estimate the effect of the environment. The CASSCF/CASPT2 calculations were performed with the MOLCAS 7.3 package.[22] The computational costs arising from the two-electron integrals were drastically reduced by employing the Cholesky decomposition (CD) technique in all CASSCF/CASPT2 calculations[23−25] combined with the local exchange (LK) screening.[26] The CASSCF/CASPT2 approach is successful in studying many actinide-containing systems.[27−30] There have also been cases in which the CASSCF/CASPT2 method has not been successful, for example, in predicting the ground state of CUO.[31] However in this case the energy difference between the possible candidates as ground state is lower than the error associated with the method (ca. 0.1−0.2 eV in energy differences when spin−orbit coupling is not included).

Results and Discussion

Cluster compositions and descriptors are reported in Figure 1, and optimized geometries are given in Tables 1−5. From geometry optimization it turned out that the uranyl groups are not symmetry-related in any of the structures.

Initially, we optimized the geometry of the $[(UO_2)_2(O_2)_5]^{6-}$ cluster (Figure 1A, structure a) without counterions (2U−P). This gave a geometrically reasonable cluster (Table 1), although the U−O_2−U dihedral angle optimized to 180° in contrast to

(11) Perdew, J. P.; Burke, K.; Ernzerhof, M. *Phys. Rev. Lett.* **1996**, *77* (18), 3865–3868.
(12) (a) Schaefer, A.; Huber, C.; Ahlrichs, R. *J. Chem. Phys.* **1994**, *100*, 5829–5835. (b) Eichkorn, K.; Weigend, F.; Treutler, O.; Ahlrichs, R. *Theor. Chem. Acc.* **1997**, *97*, 119–124.
(13) Cao, X. Y.; Dolg, M. *J. Chem. Phys.* **2001**, *115* (16), 7348–7355.
(14) Eichkorn, K.; Weigend, F.; Treutler, O.; Ahlrichs, R. *Theor. Chem. Acc.* **1997**, *97* (1−4), 119–124.
(15) Schaefer, A.; Huber, C.; Ahlrichs, R. *J. Chem. Phys.* **1994**, *100* (8), 5829–5835.
(16) Ahlrichs, R.; Bar, M.; Haser, M.; Horn, H.; Kolmel, C. *Chem. Phys. Lett.* **1989**, *162* (3), 165–169.
(17) Roos, B. O.; Taylor, P. R.; Siegbahn, P. E. M. *Chem. Phys.* **1980**, *48* (2), 157–173.
(18) Andersson, K.; Malmqvist, P.-Å.; Roos, B. O. *J. Chem. Phys.* **1992**, *96* (2), 1218–1226.
(19) Hess, B. A. *Phys. Rev. A* **1986**, *33* (6), 3742–3748.
(20) Roos, B. O.; Lindh, R.; Malmqvist, P. Å.; Veryazov, V.; Widmark, P. O. *J. Phys. Chem. A* **2005**, *109* (29), 6575–6579.
(21) (a) Gagliardi, L.; Roos, B. O. *Chem. Phys. Lett.* **2000**, *331*, 229–234. (b) Hagberg, D.; Karlstrom, G.; Roos, B. O.; Gagliardi, L. *J. Am. Chem. Soc.* **2005**, *127*, 14250–14256.
(22) Karlström, G.; Lindh, R.; Malmqvist, P.-Å.; Roos, B. O.; Ryde, U.; Veryazov, V.; Widmark, P.-O.; Cossi, M.; Schimmelpfennig, B.; Neogrady, P.; Seijo, L. *Comput. Mater. Sci.* **2003**, *287*, 222–239.
(23) Aquilante, F.; Gagliardi, L.; Pedersen, T. B.; Lindh, R. *J. Chem. Phys.* **2009**, *130*, 154107.
(24) Aquilante, F.; Pedersen, T. B.; Lindh, R.; Roos, B. O.; De Meras, A. S.; Koch, H. *J. Chem. Phys.* **2008**, *129* (2), 024113.
(25) Aquilante, F.; Malmqvist, P. A.; Pedersen, T. B.; Ghosh, A.; Roos, B. O. *J. Chem. Theory Comput.* **2008**, *4* (5), 694–702.
(26) Aquilante, F.; Pedersen, T. B.; Lindh, R. *J. Chem. Phys.* **2007**, *126* (19), 194106.
(27) (a) Gagliardi, L.; Roos, B. O. *Chem. Soc. Rev.* **2007**, *36*, 893–903. (b) Gagliardi, L. *J. Am. Chem. Soc.* **2003**, *125*, 7504–7505.
(28) La Macchia, G.; Brynda, M.; Gagliardi, L. *Angew. Chem., Int. Ed.* **2006**, *45*, 6210–6213.
(29) Gagliardi, L.; Heaven, M. C.; Krogh, J. W.; Roos, B. O. *J. Am. Chem. Soc.* **2005**, *127*, 86–91.
(30) Gagliardi, L.; La Manna, G.; Roos, B. O. *Faraday Discuss.* **2003**, *124*, 63–68.
(31) Roos, B. O.; Widmark, P. O.; Gagliardi, L. *Faraday Discuss.* **2003**, *124*, 57–62.

Table 1. Most Significant Structural Parameters of Some of the Clusters Examined, Having Na as a Counterion[a]

	distance (Å)					angle (deg)	
cluster	U−O uranyl	U−O per	O−O per	U−U	O−O uranyl−uranyl	UOOU	OUO uranyl
2U−P−Ox	1.821	2.450	1.434	4.685	4.889	180.0	175.7
2U−P−Na	1.896−1.953	2.509−2.366	1.477	4.414	3.140−5.592	144.7	173.9−174.6
2U−OH−Na	1.950−1.964	2.433−2.471	2.603	4.160	3.974−4.102	178.5	174.5−174.6
2U−OH−Ox−Na	1.864−1.865	2.331−2.359	2.343	4.063	5.009−5.012	179.9	150.5
2U−P−Ox−Na	1.831−1.840	2.325−2.343	1.435	4.065	3.143−5.924	132.1	164.0−164.4
5U−P−Ox−Na	1.801−1.889	2.362−2.456	1.448−1.477	4.119−4.242	2.832−5.691	134.5−139.6	172.7−177.7

[a] When two values are reported, they represent the shortest and longest ones, respectively.

experimentally determined values. Insertion of six Na counterions into this cluster (2U−P−Na), together with full geometry optimization, gave longer bond lengths within the cluster and an optimized U−O_2−U dihedral angle of 145°. Constraining the dihedral angle to 180° and reoptimizing the geometry of the cluster increased the energy by about 20 kcal/mol. We also determined the energy difference between the planar and bent structures for 2U−OH−Na. The structure with a dihedral angle of 160° is 2 kcal/mol higher in energy than the planar structure, and the structure with a dihedral angle of 140° is 6 kcal/mol higher in energy than the planar structure. In the 2U−OH−Na case, the energy difference between planar and bent is thus less enhanced than in the 2U−P−Na case. Optimization of the geometry of the $[(UO_2)(O_2)_2(OH)]_2^{6-}$ cluster (Figure 1A, structure b) with six Na counterions added (2U−OH−Na) resulted in a distance between the OH groups of the shared edge of 2.603 Å and a U−$(OH)_2$−U dihedral angle of about 180°. Addition of two H_2O groups to the cluster (2U−OH−Na−H_2O) did not appreciably change the optimized geometry of the cluster and again gave a U−$(OH)_2$−U dihedral angle of 180°. The geometry of the cluster $[(UO_2)_2(O_2)(C_2O_4)_4]^{6-}$ (Figure 1A, structure c), with the addition of six Na counterions, was optimized (2U−P−Ox−Na). The resulting bond lengths are reasonable although the uranyl ion is more bent than normal (Table 1). The optimized U−O_2−U dihedral angle is 132°. For comparison, the peroxide group was replaced by two hydroxyl groups and the geometry was reoptimized (2U−OH−Ox−Na). The optimized bond lengths of this hypothetical cluster are reasonable, but the uranyl ions (OUO) are unreasonably bent at 151°. The U−$(OH)_2$−U dihedral angle was 180°.

The cluster $[(UO_2)(O_2)(C_2O_4)]_5^{10-}$ (Figure 1A, structure d) was optimized with 10 added Na counterions (5U−P−Ox−Na). The geometry has reasonable bond lengths and uranyl ion angles ranging from 173° to 178°. It contains five peroxide groups that bridge between uranyl ions, and the optimized cluster has U−O_2−U dihedral angles of 135−140°.

In Table 1 we also report the U−U and O−O (uranyl−uranyl) distances. There is clearly a correlation between the O−O (uranyl−uranyl) and the UOOU dihedral angle: for the cases in which the angle is close to 180°, the O−O (uranyl−uranyl) distance is larger than the shortest O−O (uranyl−uranyl) distance for the cases in which the dihedral is bent. One can rationalize this trend as follows: in 2U−P−Ox, with no counterions and a total charge of −6, the planar structure corresponds to the least repulsion among the charges in excess. In 2U−P−Na, 2U−P−Ox−Na, and 5U−P−Ox−Na, the bending of the dihedral angle, which is possible because the presence of the bridging peroxo ensures the maximum Coulombic attraction between the uranyl oxygens and the counterions. In 2U−OH−Na and 2U−OH−Ox−Na, on the other hand, the OH groups, unlike the peroxo group, do not play a bridging role and they do not favor bending.

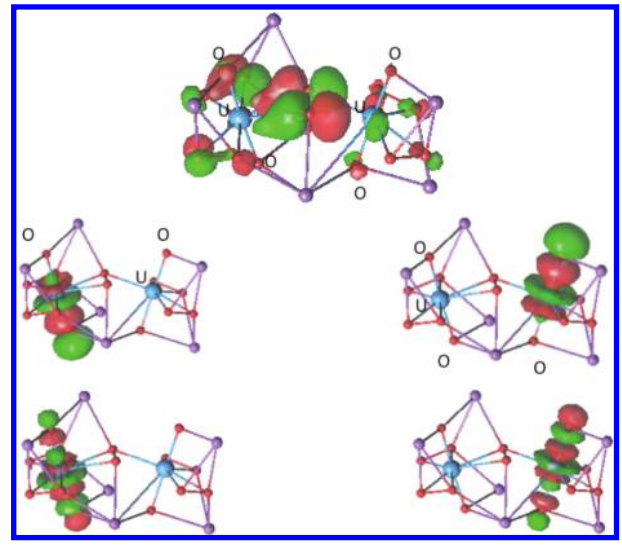

Figure 2. Selected molecular orbitals responsible for the bonds in cluster 2U−P−Na. The upper orbital shows the covalent interaction between the central peroxo and the two U atoms. The other four orbitals are those in the HOMO−LUMO region and they are entirely uranyl-based. U, blue; O, red; Na, purple.

We performed a full characterization of the wave function in the case of 2U−P−Na in order to better understand the electronic structure of this species and provide insight concerning the origin of the bent U−O_2−U interactions. The optimized cluster 2U−P−Na has a U−O_2−U dihedral angle of 145°. Projections of selected molecular orbitals, from a CASSCF/CASPT2 calculation, responsible for the bonds present in this cluster are shown in Figure 2. The calculation revealed the presence of a bonding molecular orbital along the U−O_{peroxo} bond, the top one in Figure 2. This orbital is a linear combination of the peroxo π along the plane and the U 6p orbitals. The 6p orbitals are usually described as corelike orbitals, so one wonders why instead the uranium 5f and 6d orbitals do not participate in the interaction with the peroxo. The reason is that the 5f and 6d orbitals are mainly involved in the interaction with the uranyl oxygens and the 6p are the next orbitals energetically available for the interaction with the peroxo and they point in the right direction. In the analogous hydroxyl cluster, 2U−OH−Na, in contrast, there is no such bonding orbital along the corresponding U−$O_{hydroxo}$ bond since there is not an analogous hydroxyl π molecular orbital of the right symmetry to be combined with the U orbitals. All orbitals on the OH−OH moiety are fully localized on each individual OH group and there is no covalent interaction between the two OH groups. Calculated partial charges for the 2U−P−Na cluster are +2.03 to +2.12 for the U cation, −0.67 to −0.99 for the O atoms of the uranyl ions, and −0.67 to −0.75 for the O atoms of the peroxide groups. The partial charges of the 2U−OH−Na−H_2O cluster are +2.16 to +2.19 for the U cation, −0.79 to −0.97 for the O atoms of

Table 2. Most Significant Structural Parameters of 2U−P−A Clusters in the Presence of Different Counterions[a]

	distance (Å)					angle (deg)	
A	U−O uranyl	U−O per	O−O per	U−U	O−O uranyl−uranyl	UOOU	OUO uranyl
Li	1.888−1.959	2.360−2.521	1.471	4.342	3.181−5.637	139.9	167.1−167.9
Na	1.895−1.947	2.369−2.502	1.472	4.397	3.110−5.614	143.6	174.0−174.5
K	1.894−1.938	2.361−2.503	1.469	4.434	3.273−5.486	147.1	175.8−176.9
Rb	1.902−1.944	2.341−2.534	1.481	4.516	3.530−5.205	155.5	172.8−176.0
Cs	1.903−1.930	2.390−2.575	1.469	4.552	3.876−5.001	164.3	175.1−177.3

[a] When two values are reported, they represent the shortest and longest ones, respectively.

the uranyl ions, and −0.91 to −0.92 for the O atoms of the hydroxyl groups. The presence of a bonding molecular orbital along the $U-O_{peroxo}$ bond, together with the observation that the O atoms of the hydroxyl group are more ionic than those of the peroxide group, confirms that there is some covalent bonding in the case of the peroxide bridge. In Figure 2 we also report the orbitals in the HOMO−LUMO region, which are mainly localized on the two uranyl moieties. These four orbitals are similar in the peroxo and hydroxo cases.

We propose that the difference in bonding along the $U-O_{peroxo}$ and $U-O_{hydroxo}$ bonds revealed by our calculations is responsible for the bent $U-O_2-U$ dihedral angle, while the $U-(OH)_2-U$ dihedral angle in the comparable cluster tends to be planar. However, recall the calculations on the 2U−P and 2U−P−Na clusters indicate that the $U-O_2-U$ dihedral angle becomes bent only when the charge of the uranyl polyhedra is balanced by counterions. A possible explanation for the bent $U-O_2-U$ dihedral angles observed experimentally and confirmed by our calculations is that the counterions in our calculations interact with the uranyl ion O atoms, making the U atoms more "available" for interactions with the equatorial O atoms of peroxide or hydroxyl groups; however, while in the peroxo-bridged cluster a $U-O_{peroxo}$ covalent bond forms. This cannot happen in the hydroxo-bridged case because the O atoms of the hydroxyl groups are polarized by the presence of the H atoms.

The argument usually advanced to explain the formation of cation−oxo ligand interactions is that strong equatorial donors increase the negative charge on the oxo ligands, thereby increasing their Lewis basicity. This was discussed in a paper by Clark et al.;[32] on the basis of their argument, the hydroxo complex should exhibit stronger uranyl interactions (over the peroxo), because it is a stronger donor. Ingram et al.[33] also discussed the same issue and showed that the Lewis basicity increases with the number of coordinated hydroxides. However, according to Ingram et al.[33] the hydroxide is not necessarily a stronger donor and peroxide forms in some complexes very short bonds with uranyl, in agreement with our interpretation of the results we obtain.

The observation that counterions are needed in our model clusters to produce bent $U-O_2-U$ dihedral angles prompted us to hypothesize that counterions may permit tuning of the $U-O_2-U$ dihedral angle. We optimized the geometries for each of the clusters under study using Li, Na, K, Rb or Cs as the counterions (designated A in the descriptors). The resulting geometries are presented in Tables 2−5. The optimized geometries of the two uranyl bipyrimid polyhedra in the simplest cluster 2U−P−A remain essentially constant despite changing

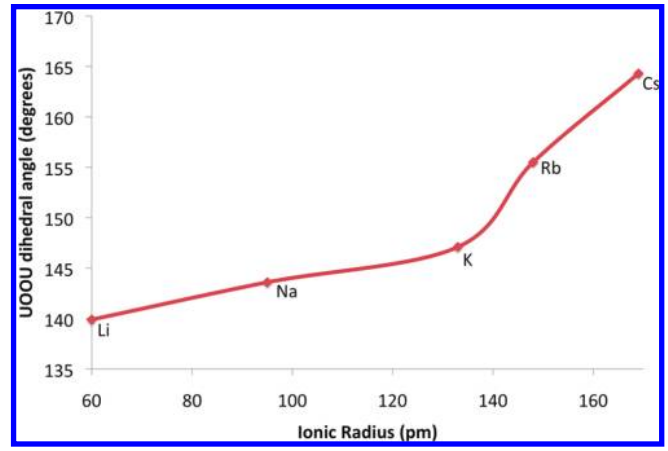

Figure 3. Peroxo dihedral angle as a function of the ionic radius[34] of the counterions in the 2U−P−A clusters.

the counterion, with the exception of the uranyl ion bond angle, which is more bent in the case of A = Li. The $U-O_2-U$ dihedral angle of the peroxo bridge steadily increases with the size (and decreasing electronegativity) of the counterion, from 140° in the case of A = Li to 164° for A = Cs. In Figure 3 we report the peroxo dihedral angle as a function of the ionic radius of the counterion for the 2U−P−A clusters. In Table 6 we report Mulliken charges for the 2U−P−A clusters for various counterions. In going from Li to Cs, the uranyls become less ionic and the O_{peroxo} more negatively charged as the UOOU dihedral angle increases.

We also determined the energy difference between the planar and bent structures for 2U−P−A, for A = Li to Cs. The energy difference between planar and bent decreases along the series, going from 37 kcal/mol for Li to 6 kcal/mol for Cs. This trend is consistent with the trend in the bending angle.

For comparison, optimized geometries for the hydroxo-bridged clusters 2U−OH−A and $2U-OH-A-H_2O$ are listed in Table 3. For 2U−OH−A the calculated geometries of the uranyl polyhedra do not differ much as the counterion is changed, except again in the case of A = Li, where the uranyl ion bond angle is more bent than the others. The $U-(OH)_2-U$ dihedral angles for the bridging hydroxo edge are 180° within uncertainty for A = Li, Na, Rb, and Cs. For A = K, the dihedral angle is 157°. We attribute the nonplanarity of the bridge to counterions bridging between two uranyl ion O atoms, which would encourage bending in a pliable system. It also seems plausible that K has the perfect ionic radius to bridge two uranyl ion oxygens.

Where two H_2O groups are added to the optimization ($2U-OH-A-H_2O$), the $U-(OH)_2-U$ dihedral angle for the

(32) Clark, D. L.; Conradson., S. D.; Donohoe, R. J.; Keogh, D. W.; Morris, D. E.; Palmer, P. D.; Rogers, R. D.; Tait, C. D. *Inorg. Chem.* **1999**, *38*, 1456–1466.
(33) Ingram, K. I. M.; Haller, L. J. L.; Kaltsoyannis, N. *Dalton Trans.* **2006**, *20*, 2403–2414.
(34) Huheey, J. E.; Keiter, E. A.; Keiter, R. L., *Inorganic Chemistry: Principles of Structure and Reactivity*, 4th ed.; HarperCollins: New York, 1993.

Table 3. Most Significant Structural Parameters of 2U−OH−A Clusters in the Presence of Different Counterions[a]

	distance (Å)					angle (deg)	
A	U−O uranyl	U−O per	O−O per	U−U	O−O uranyl−uranyl	UOOU	OUO uranyl
Li	1.976	2.405−2.406	2.63	4.028	3.642−3.645	180.0	168.8−168.9
Na	1.950−1.964	2.420−2.458	2.595	4.135	3.941−4.077	178.3	174.5−174.6
K	1.925−1.940	2.416−2.525	2.544	4.143	3.410−4.754	156.8	176.6−178.4
Rb	1.923−1.938	2.410−2.531	2.774	4.112	3.780−4.025	177.4	172.5−174.2
Cs	1.920−1.933	2.426−2.517	2.75	4.079	3.823−3.925	179.6	173.2−174.1

[a] When two values are reported, they represent the shortest and longest ones, respectively.

Table 4. Most Significant Structural Parameters of 2U−P−Ox−A Clusters in the Presence of Different Counterions[a]

	distance (Å)					angle (deg)	
A	U−O uranyl	U−O per	O−O per	U−U	O−O uranyl−uranyl	UOOU	OUO uranyl
Li	1.831−1.922	2.306−2.519	1.443	3.818	2.899−5.884	115.4	155.4−173.6
Na	1.832−1.840	2.322−2.353	1.431	4.060	3.170−5.848	131.9	164.8−165.1
K	1.833−1.839	2.349−2.362	1.433	4.324	3.695−5.568	149.0	170.0−170.2
Rb	1.833−1.838	2.356−2.363	1.435	4.479	4.499−5.044	170.6	170.8−170.9
Cs	1.831−1.839	2.369−2.375	1.435	4.494	4.337−5.156	167.0	171.8−172.3

[a] When two values are reported, they represent the shortest and longest ones, respectively.

Table 5. Most Significant Structural Parameters of 5U−P−Ox−A Clusters in the Presence of Different Counterions[a]

	distance (Å)					angle (deg)	
A	U−O uranyl	U−O per	O−O per	U−U	O−O uranyl−uranyl	UOOU	OUO uranyl
Li	1.798−1.858	2.300−2.440	1.441−1.480	4.088−4.170	2.648−5.903	129.5−132.6	172.8−177.0
Na	1.802−1.865	2.316−2.452	1.442−1.474	4.121−4.240	2.830−5.689	134.5−139.4	173.7−177.8
K	1.819−1.864	2.318−2.453	1.444−1.468	4.282−4.448	3.163−5.585	143.1−158.7	173.9−179.0
Rb	1.825−1.866	2.332−2.451	1.446−1.465	4.346−4.467	3.400−5.479	148.6−157.5	173.5−178.2
Cs	1.834−1.864	2.333−2.471	1.448−1.462	4.418−4.475	3.714−5.231	157.0−158.7	174.4−176.9

[a] The two values reported represent the shortest and longest ones, respectively.

Table 6. Mulliken Charges Calculated at the PBE/def-TZVP Level of Theory for 2U−P−A Clusters for Various Counterions[a]

	Li	Na	K	Rb	Cs
U	+0.94 to +1.02	+0.62 to +0.68	+0.64 to +0.69	+0.60 to +0.70	+0.55 to +0.64
O_{yl}	−0.67 to −0.47	−0.69 to −0.53	−0.69 to −0.52	−0.68 to −0.54	−0.64 to −0.56
O_{peroxo}	−0.36 to −0.34	−0.44 to −0.34	−0.45 to −0.340	−0.46 to −0.41	−0.41 to −0.37

[a] When two values are reported they represent the largest and smallest charge, respectively.

bridging hydroxo edge is 180° within uncertainty for A = Li and Na. For A = K, Rb, and Cs, the dihedral angles are 153°, 161° and 170°, respectively.

Optimizations for the 2U−P−Ox−A clusters (Table 4) result in generally reasonable polyhedral geometries with the exception of the uranyl ion bond angles, which are more bent than expected. The $U-O_2-U$ dihedral angles of the peroxo bridge steadily increase with the size of the counterion, ranging from 115° for A = Li to 171° for A = Rb and 167° for A = Cs. Calculations for the hypothetical 2U−OH−Ox−A cluster provided optimized geometries that are generally incompatible with those expected from experimental studies of other clusters, with O−O distances between hydroxyl groups being too short and uranyl ion bonds departing too far from linearity. We emphasize that this cluster has not been obtained experimentally. Despite the shortcomings in the polyhedral geometries, the $U-(OH)_2-U$ dihedral angles for the bridging hydroxo edge are 180° within uncertainty for A = Na, K, Rb, and Cs. In the case of A = Li, the dihedral angle is 150°.

Geometric parameters for the optimized 5U−P−Ox−A clusters are reported in Table 5. There are five uranyl ions that share five peroxo bridges, forming a pentagonal ring. The calculated bond lengths and angles of the uranyl bipyramids are consistent with experimentally derived values and differ only slightly with the identity of the counterion present. In contrast, the $U-O_2-U$ dihedral angles vary considerably and systematically with the ionic radii of the counterions, from 129−133° for A = Li to 157−158° for A = Cs. In other words, increasing the size of the counterion associated with the five-membered ring significantly flattens the overall structure.

Conclusions

Formation of closed clusters of uranyl peroxide polyhedra is spontaneous in aqueous solutions under ambient conditions, and such clusters can persist for months in solution.[2−7] Their topologies are highly complex, containing 20−60 uranyl ions. There are many possible topologies for the clusters, including fullerene topologies and some that contain topological squares. Three fundamental questions have arisen concerning these nanoscale clusters and their self-assembly in solution:

(1) What factor(s) cause the polyhedra to assemble into nanostructures rather than into conventional extended structures?

(2) Why do clusters with different sizes assemble, currently ranging from 20 to 60 uranyl polyhedra?

(3) For a given number of vertices, what determines which topological isomer is selected?

We have recently concluded that isomer selection is dominated by symmetry.[5,7] Specifically, for a given number of uranyl polyhedra, the cluster with the highest possible symmetry (excluding those that would require unreasonable edges) will

form because this is compatible with the most even distribution of any strain associated with the required curvature. Our calculations now allow us to address the first two questions. All electroneutral clusters containing a peroxo bridge between uranyl bipyramids have strongly bent $U-O_2-U$ dihedral angles. The corresponding $U-(OH)_2-U$ dihedral angle in model clusters tends to be flat, although a bent angle is not prohibited. It is the covalent interaction that extends along the $U-O_{peroxo}$ bonds that causes the $U-O_2-U$ dihedral angle to be bent, and it is this inherent bending of the configuration that encourages curvature and cage cluster formation. Our calculations have also shown that the $U-O_2-U$ dihedral angle of the peroxo bridge is tuned by the size or electronegativity of the counterion present. In other words, different counterions favor different *degrees of curvature*, which is reflected in the range of cluster sizes.

Acknowledgment. This research was supported by Director, Office of Basic Energy Sciences, U.S. Department of Energy under Contract USDOE/DE-SC002183, and the Materials Science of Actinides Center, an Energy Frontier Research Center funded by the U.S. Department of Energy, Office of Science, Office of Basic Energy Sciences under Award DE-SC0001089.

Supporting Information Available: Forty-two tables, listing coordinates of the optimized structures. This material is available free of charge via the Internet at http://pubs.acs.org.

JA104964X